



Cloud Condensation Nuclei Activity and Hygroscopicity of Fresh and Aged Biomass Burning Particles

YANWEI LI¹

Abstract—Biomass burning particles are one of the largest aerosol sources worldwide and contribute a significant fraction of the global cloud condensation nuclei (CCN) burden. Chemical aging experiments of sawgrass burning particles took place in a smog chamber by turning on the UV light after HONO or H₂O₂ injection. The CCN activity and corresponding hygroscopicity of fresh and aged particles were measured. Most of the fresh particles can serve as reasonable CCN, and the average activation diameters at 0.2% supersaturation were 114–125 nm in the experiments. The aging process caused that the mass fraction of organic aerosols decrease and condensed phase nitrate NO₃[−] increase, and also the average atomic oxygen to carbon (O:C) ratios increase, which were the main reasons that the aged particles were more CCN active and hygroscopic. The average activation diameters decreased by 8–15% at 0.2% supersaturation after aging, and hygroscopic parameter κ increased by 30–42%. The chemical aging productions were a little different in experiments, but the CCN property and hygroscopicity change trends were quite similar.

Key words: Biomass burning particles, hygroscopic properties, CCN, chemical aging.

1. Introduction

Atmospheric aerosol particles serving as cloud condensation nuclei (CCN) are very important elements of the hydrological cycle and climate (Rose et al. 2010) because aerosol particles change cloud microphysical structures and radiative properties (Xu 2001; Zhao et al. 2006; Li et al. 2007; Rosenfeld et al. 2017). Under increasing aerosol number concentrations, clouds tend to have more, but smaller droplets, and thus reflect more solar radiation (Twomey 1977).

Aerosol and cloud interactions directly influence the cloud microphysical process, thus leading to changes of spatio-temporal distribution of precipitation, rather than on the globally-averaged amount of precipitation (Rosenfeld et al. 2008). Gultepe and Isaac (1999) and Gultepe et al. (2017) stated that no unique relationship exists between aerosols and cloud particles unless variability is considered, and their influence for precipitation is quite uncertain.

Biomass burning from open vegetation fires and domestic wood burning for heating or cooking is one of the largest aerosol sources worldwide (Martin et al. 2013), and contributes a significant fraction of the global CCN burden (Pierce et al. 2007; Andreae 2009; Spracklen et al. 2011). Biomass burning injects particles into the air and may cause CCN concentration outbursts in regions, such as Amazonia, sub-Saharan Africa (Andreae and Rosenfeld 2008; Andreae 2009; Hennigan et al. 2012), Alpine valleys (Sandradewi et al. 2008; Szidat et al. 2007), Zurich (Lanz et al. 2008), Paris (Favez et al. 2009), Beijing (Duan et al. 2004), Guangzhou (Rose et al. 2010), Austria (Caseiro et al. 2009), and the eastern Mediterranean (Bougiatioti et al. 2016).

Most of the aerosol particles from biomass burning are in the sub-micrometer size range. Because of their small sizes, fire plumes are often transported for thousands of kilometers and reside for a long time in the atmosphere (Li et al. 2003; Anderson et al. 1996). Fresh biomass burning particles consist mainly of organic material (OM), black carbon (BC), and some inorganic components (Reid et al. 2005). Because of their chemical composition, biomass burning particles can be CCN active even though they are aerosols in dark color, and their properties change during the long transportation in the atmosphere, which

¹ Collaborative Innovation Center on Forecast and Evaluation of Meteorological Disasters, Key Laboratory for Aerosol-Cloud-Precipitation of China Meteorological Administration, Nanjing University of Information Science and Technology, Nanjing, China. E-mail: liyw@nuist.edu.cn

influences the hygroscopicity of particles (Decesari et al. 2002; Zuberi et al. 2005; Martin et al. 2013).

Biomass burning particles from open fire events were studied and results showed the particles size distribution, composition, optical properties and hygroscopicity in some areas, such as Brazil, Yucatan Peninsula, Amazonian, northern Australia, Beijing, Guangzhou and so on (Kaufman et al. 1998; Lee et al. 2006; Vestin et al. 2007; Mallet et al. 2017; Wu et al. 2016; Rose et al. 2010).

The CCN activities and hygroscopic properties of fresh biomass burning particles from more than twenty kinds of biomass fuels were investigated through the experiments conducted under controlled laboratory conditions by several groups (Dusek et al. 2005; Novakov and Corrigan 1996; Petters et al. 2009; Engelhart et al. 2012; Martin et al. 2013). Their results show the fresh particles had a broad range of hygroscopicity and some kinds are hygroscopic and water soluble, exhibiting up to about half the water uptake capacity of ammonium sulfate; different size particles contain different components, causing different CCN activities and hygroscopicity.

The CCN activities and hygroscopic properties of aged biomass burning particles from several kinds of fuels were also detected in some chamber experiments. Engelhart et al. (2012) found that photochemical aging process could increase or decrease hygroscopicity of the particles, depending the chemical components. Martin et al. (2013) found that the hygroscopicity of the wood burning particles generally increased with aging. Hennigan et al. (2012) found secondary organic aerosol production caused new particles to grow rapidly, significantly enhancing CCN concentrations in aging process.

Previous studies supplied a lot of results, but most studies have focused more on the fresh particles and less on aged particles (Pratt et al. 2010); however, the particles may differ substantially from exposure to oxidants or condensable gases over periods ranging from hours to weeks (Hobbs et al. 2003; Lee et al. 2006) during the transport process from the original sources (Capes et al. 2008; Hennigan et al. 2011, 2012). More observations or experiments should be done related to aged biomass burning particles. In this study, we measured the CCN activities and hygroscopicity of biomass burning

particles produced from saw grass. After the characterization of the fresh particles, the emissions were exposed to H₂O₂ or HONO, and then the UV light was turned on, to simulate chemical aging. The composition of the fresh and aged particles was characterized through aerosol mass spectrometry (AMS). The CCN activity and hygroscopic properties were measured by CCN counter (CCNC) along with scanning mobility particle sizer (SMPS).

2. Hygroscopic Parameter κ

Petters and Kreidenweis (2007, 2008) used a hygroscopic parameterization κ , to parameterize the hygroscopic properties of particles, as in Eq. 1. Higher values of κ means more-hygroscopic, while lower values of κ then indicate less-hygroscopic.

$$S = \frac{D_p^3 - D_s^3}{D_p^3 - D_s^3(1 - \kappa)} \exp\left(\frac{4\sigma M_w}{RT\rho_w D_p}\right), \quad (1)$$

where S is the water vapor saturation relative to a flat pure water surface, M_w is the molecular weight of water, σ is the surface tension of the solution, R is the gas constant, T is the temperature, ρ_w is the density of water, D_p is the droplet diameter, D_s is the diameter of the dry particle.

κ can be derived from Eq. 1, and if κ is larger than 0.2, it can be calculated by Eqs. 2 and 3.

$$\kappa = \frac{4A^3}{27D_{sc}^3 \ln^2 S_c}, \quad (2)$$

$$A = \frac{4M_w\sigma}{RT\rho_w}. \quad (3)$$

In which, S_c is the critical saturation and D_{sc} is the activation diameter.

3. Experimental Descriptions

The experimental setup used in this study is shown in Fig. 1. The experiments were carried out in the environmental smog chamber in the Air Quality Laboratory of Carnegie Mellon University. The smog chamber is a 10 m³ Teflon reactor (Welch Fluorocarbons) inside a temperature controlled room. The

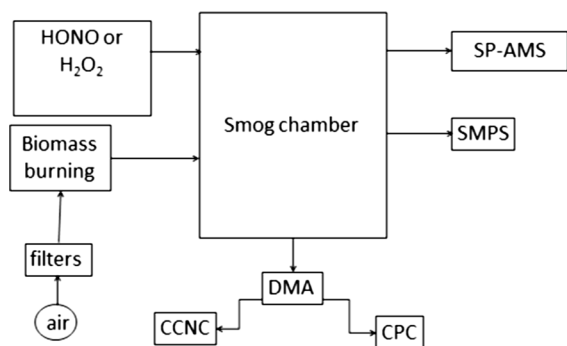


Figure 1
Experimental setup used in this study

walls of the smog chamber room are lined with UV lights (General Electric model 10526 black). Prior to an experiment, the chamber was flushed with purified air for 12–48 h. Air was passed through HEPA and carbon filters to remove particles and gas-phase organics, respectively and silica gel to reduce the relative humidity (RH). All of the experiments were carried out at a constant temperature of 20 ± 2 °C and at a RH < 10%.

The dried saw grass was burned and the particles were injected into the smog chamber using two ejector diluters (Dekati, Finland) in parallel. The fresh particles were observed for 2 h in the smog chamber. The aging of particles was initiated by either turning on the UV lights after 10 min of the HONO injection (Experiment 1) or half an hour after the H₂O₂ injection (Experiment 2) after the fresh particles injection. The aged particles were observed for at least 6 h.

The CCN activity of burning grass particles was measured with a continuous-flow streamwise thermal-gradient CCN counter (CCNC, DMT) (Roberts and Nenes 2005). In these experiments, we used the CCNC coupled to a SMPS (TSI, classifier model 3080, CPC model 3772) to measure the CCN concentration at different sizes using the scanning mobility CCN analysis (SMCA). A differential mobility analyzer (DMA) was placed in front of the CCNC and CPC (Moore et al. 2010). The sample stream passed through the DMA and then the stream was split into two streams; one entered the CPC and the other one entered the CCNC. Using SMCA, the ratio between the CCN number concentration and

particle number concentration (CCN/CN) can be measured as a function of particle size.

During the experiments, the sample airflow to the DMA was 0.8 L min^{-1} . The CCNC total airflow was 0.5 L min^{-1} , and the CPC sample flow was 0.3 L min^{-1} . The DMA sheath flow was set to 4 L min^{-1} in order to get broader size distributions. A 120 s voltage upscan and a 15 s voltage downscan for the DMA were used. Before the experiments, the CCNC was calibrated with ammonium sulfate following the procedure of Rose et al. (2008) and Engelhart et al. (2008).

A second SMPS was sampling directly from the smog chamber. The sample flow rate was 0.3 L min^{-1} and the sheath flow rate was 3 L min^{-1} . The voltage upscan time was 120 s and the voltage downscan time was 30 s.

A Soot Particle Aerosol Mass Spectrometer (SP-AMS, Aerodyne Research, Inc.) was used to monitor the mass concentration and the chemical composition of the particles (Jayne et al. 2000; Jimenez et al. 2003; Onasch et al. 2012). The SP-AMS uses laser-induced incandescence of absorbing soot particles to vaporize both the coatings and elemental carbon cores within the ionization region of the AMS, providing a unique and selective method for measuring the mass of the refractory carbon cores (i.e., black carbon mass), the mass and chemical composition of any coating material (e.g., organics, sulfates, nitrates, etc.), and particle size. In our analysis, the elemental ratios (O:C) of the particles were calculated using the algorithms suggested by Aiken et al. (2008).

4. Experimental Results

Two chemical aging experiments of burning sawgrass particles were conducted by turning on the UV lights after HONO (Experiment 1) or H₂O₂ (Experiment 2) injection. The CCN activity and hygroscopic properties were measured right after the smog chamber was filled with fresh particles.

The experimental setup described above was used to measure the activation ratio (CCN/CN) at the water supersaturation of the CCNC. Constant supersaturations of 0.2 and 0.4% were used in Experiment 1 and 0.2% in Experiment 2. For each

supersaturation, the activation diameter was defined as the diameter where CCN/CN was equal to 0.5 (Cruz and Pandis 1997).

4.1. Size Distribution of Burning Grass Particles

Based on SMPS results, after injection into the chamber for Experiment 1, the aerosol number concentration increased rapidly to around $71,500 \text{ cm}^{-3}$, with a number mode diameter of 74 nm (Fig. 2a), and then decreased because of losses to chamber wall. When the UV lights were turned on after HONO injection, the aerosol concentration increased fast because of nucleation causing new particle formation (NPF). During NPF time period and after that, particles did not exhibit a

unimodal distribution. There were two peaks for the number concentration at two different sizes. At 14:31, one was $1,980,000 \text{ cm}^{-3}$, with a number mode diameter of 13.6 nm, corresponding to the NPF; the other one was $19,003 \text{ cm}^{-3}$, with a number mode diameter of 109.4 nm, corresponding to the original particles, and the increasing of number mode diameter implied condensation process causing the original particles to grow bigger. After that, the number concentration dropped down very fast again because of wall loss and coagulation of newly-formed small particles. By the end of the experiment at 24:00, one peak number concentration was around 1976 cm^{-3} , with a number mode diameter of 44.5 nm, and the other one was 5384 cm^{-3} , with a number mode diameter of 174.7 nm.

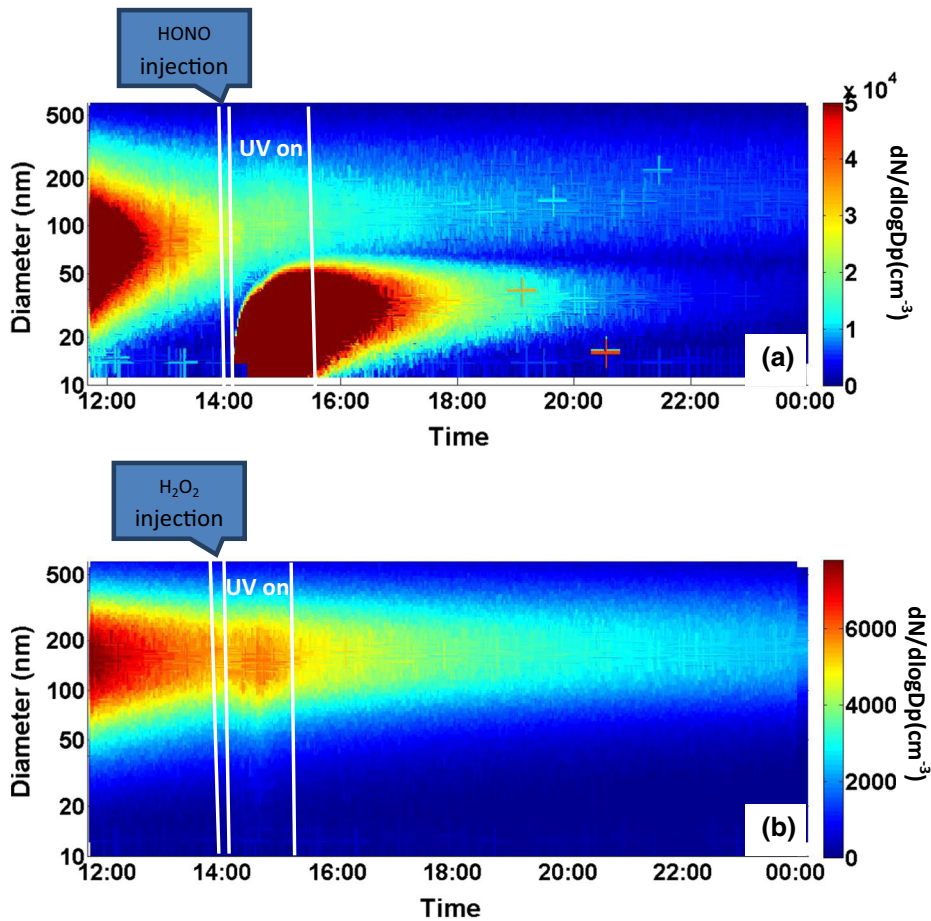


Figure 2
Number distribution of **a** Experiment 1 and **b** Experiment 2

The fresh aerosol number concentration (Fig. 2b) changed similar in Experiment 2 with those in Experiment 1 because of wall loss until beginning of aging process. During aging process in Experiment 2, there was no evident NPF due to nucleation, but there was a condensation process causing original particles to grow bigger. The peak number concentration changed from 7258 cm^{-3} , with a number mode diameter of 141 nm at 12:00 to 5740 cm^{-3} , with a number mode diameter of 146 nm at 14:55 right before the UV light was turned off.

4.2. Chemical Aging of Burning Grass Particles

As measured by the SP-AMS, the initial organic aerosol (OA) mass concentration was approximately $98 \mu\text{g m}^{-3}$, while NO_3^- and the black carbon (BC) mass concentration were approximately 3.3 and $7.7 \mu\text{g m}^{-3}$, respectively (Fig. 3a), in Experiment 1.

The concentrations of the other chemical components of the particles were negligible ($< 0.5\%$). The concentration of the OA and BC decreased rapidly due to wall losses in the smog chamber. While the UV lights were turned on, the chemical aging process led to the immediate increase of OA and NO_3^- , which reached a maximum of $56.3 \mu\text{g m}^{-3}$ for OA at 14:50 and $6.3 \mu\text{g m}^{-3}$ for NO_3^- at 15:30. The BC mass concentration always decreased during the whole experiment.

Figure 3b shows the time series of mass fraction for BC, OA, and NO_3^- in Experiment 1, which showed that all three main components kept stable mass fraction before aging. After aging, the OA mass fraction decreased from 89 to 84%, while the NO_3^- increased from 4 to 13%. BC dropped down from 6 to 0%.

The time series of mass concentration and mass fraction of Experiment 2 were quite similar with

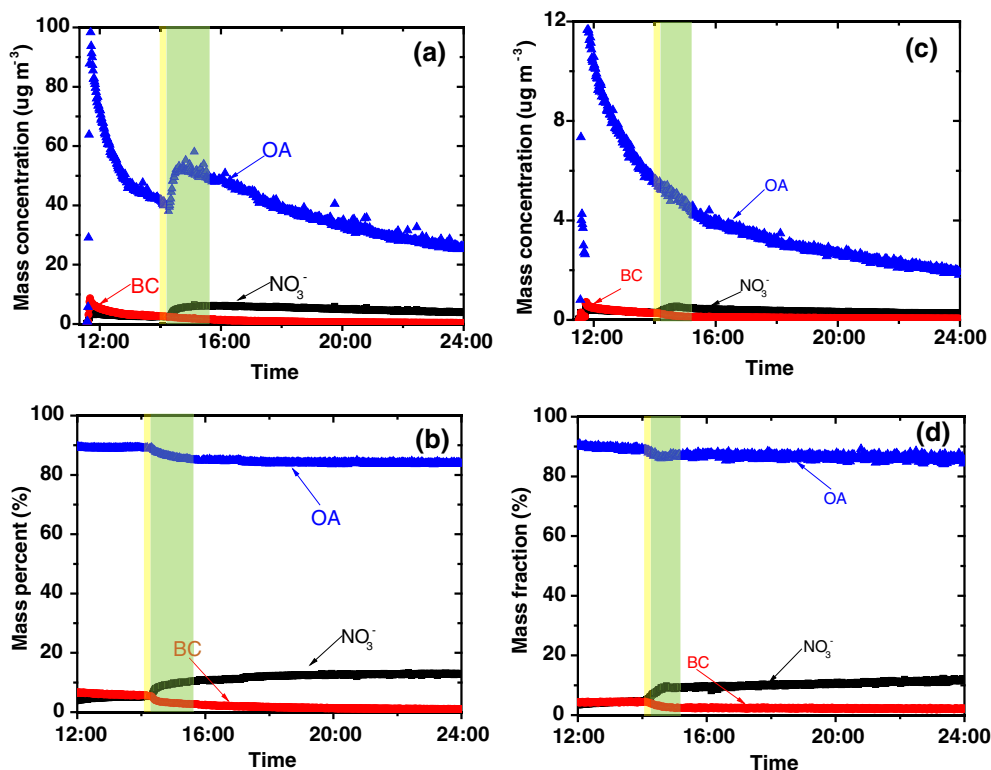


Figure 3

The time series of mass concentration in **a** Experiment 1, **c** Experiment 2 and mass fraction in **b** Experiment 1, **d** Experiment 2 for the organic aerosol (OA), NO_3^- , and black carbon (BC). The yellow shadow means **a, b** HONO and **c, d** H_2O_2 injection, and the green shadow means the UV light was turned on

those of Experiment 1 (Fig. 3c, d). For the main chemical components, the mass fraction of OA decreased and NO_3^- increased which might cause the hygroscopic feature of the particles to change.

The elemental ratios of the burning grass particles calculated using the SP-AMS measurements are shown in Fig. 4a, b. The O:C ratio of the particles in Experiment 2 was higher than in Experiment 1, while both of them increased upon aging. For example, in Experiment 1, the fresh particles emissions had an O:C ratio equal to 0.28, while the chemical aging of the particles resulted in an increase of the O:C ratio by approximately 50 to 0.41% (Fig. 3). This meant that OA in the aerosols became more oxidized and expected to be more hygroscopic.

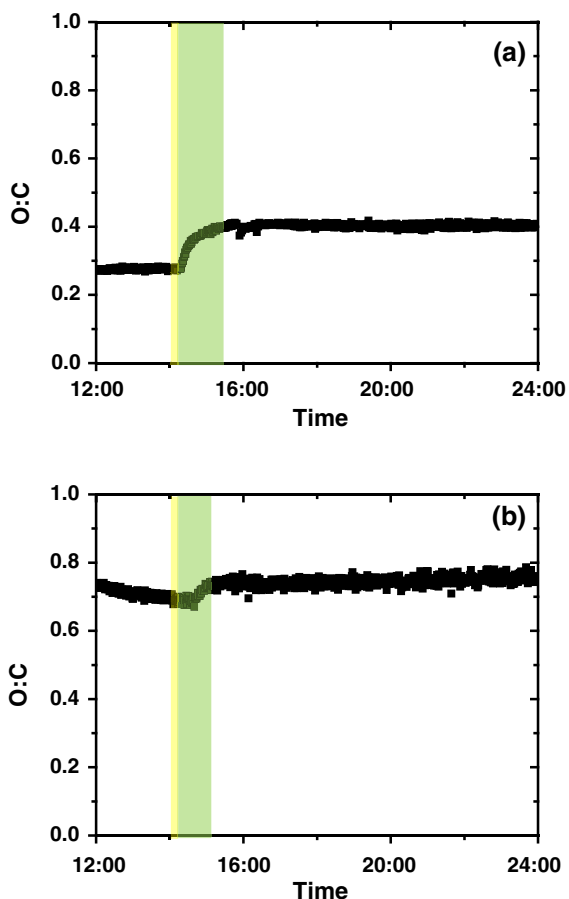


Figure 4

O:C ratios calculated using Aiken et al. (2008) method for a Experiment 1 and b Experiment 2. The yellow shadow means a HONO and b H_2O_2 injection, and the green shadow means the UV light was turned on

4.3. CCN Activity

The fresh particles from Experiment 1 were CCN active because they contain some water soluble components. The average activation ratio for fresh particles was 39% at 0.2% supersaturation and 68% at 0.4% supersaturation (Fig. 5a). The particles became more CCN active after aging, although the fraction of CCN active particles decreased immediately following the aging process because of nucleation leading to new smaller particles formation, but it rapidly increased again after NPF following the aging process. The particles activated at 0.2% supersaturation increased from 37 to 76% and from 60 to 82% at 0.4% supersaturation in a few hours. The activation ratio results changed slightly in Experiment 2 (Fig. 5b), it increased much less and remained more stable than those in Experiment 1 because there was no nucleation occurring.

The average activation diameter was 114 nm at 0.2% supersaturation and 67 nm at 0.4% supersaturation in Experiment 1 (Fig. 5c). After aging, the activation diameter at 0.2% supersaturation decreased from 114 to 88 nm and from 67 to 61 nm at 0.4% supersaturation in this experiment. The activation diameter was a little larger in Experiment 2 (Fig. 5d) than that in Experiment 1, but the overall trends were similar in both experiments.

The change in CCN activity for both experiments was consistent with the chemical changes of the particles (Figs. 2 and 3). For example, in Experiment 1, when the UV lights were turned on, the OA mass fraction decreased, but O:C ratio increased, meaning stronger oxidation extent. At the same time, the NO_3^- fraction increased very fast. The aging process changed the chemical composition of the particles, which caused the particles to become more CCN active.

The activation diameters of the fresh and aged particles are compared in Fig. 6. In both experiments, the fresh particles were less active than the aged particles. This suggests that the changes due to aging allowed many smaller particles to become more effective CCN.

From Figs. 5 and 6, we found that two experiments showed particles had similar CCN active diameters initially and decreased upon aging, despite

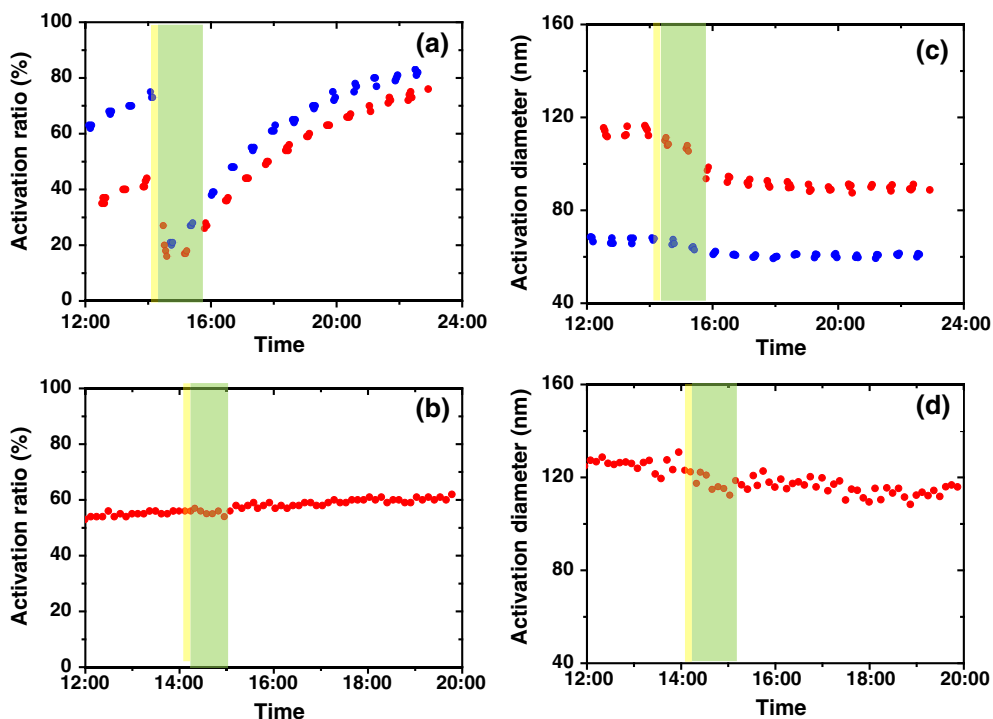


Figure 5

Time series of **a** activation ratio and **c** activation diameter for Experiment 1; **b** activation ratio and **d** activation diameter for Experiment 2. The yellow shadow means **a** and **c** HONO, **b** and **d** H₂O₂ injection. The green shadow means the UV lights were turned on. The red points correspond to results at supersaturation 0.2% and blue points correspond to 0.4%



Figure 6

Average activation diameter and its standard deviation for the fresh and aged particles (the 5th and 6th hours after aging) at 0.2% supersaturation in the CCNC

nucleation occurring in only one of these experiments. Additionally, CCN activity changes seemingly correlate to a decrease in OA fraction, increase in NO₃⁻, and increase in O:C ratio. CCN activity

results were generally similar, even though the chemical aging productions were different, with one including evident nucleation and the other one not.

4.4. Hygroscopicity Parameter, κ

The hygroscopicity parameter, κ , can be calculated using Eqs. 1–3. A surface tension of 72 dyn cm⁻¹ has been used to estimate κ in this work, and the results were shown in Figs. 7 and 8.

The κ for the fresh particles were smaller. In Experiment 1, the average κ of fresh particles was 0.24 and that of aged particles increased by 42 to 0.34% (Fig. 7a). The κ changed more slowly in Experiment 2 than those in Experiment 1, but still increased by 30%, from 0.17 to 0.23 (Fig. 7b).

Even though the κ increase amounts were different between two experiments, while the trends were quite similar, chemical aging caused particles to become more hygroscopic (Fig. 8).

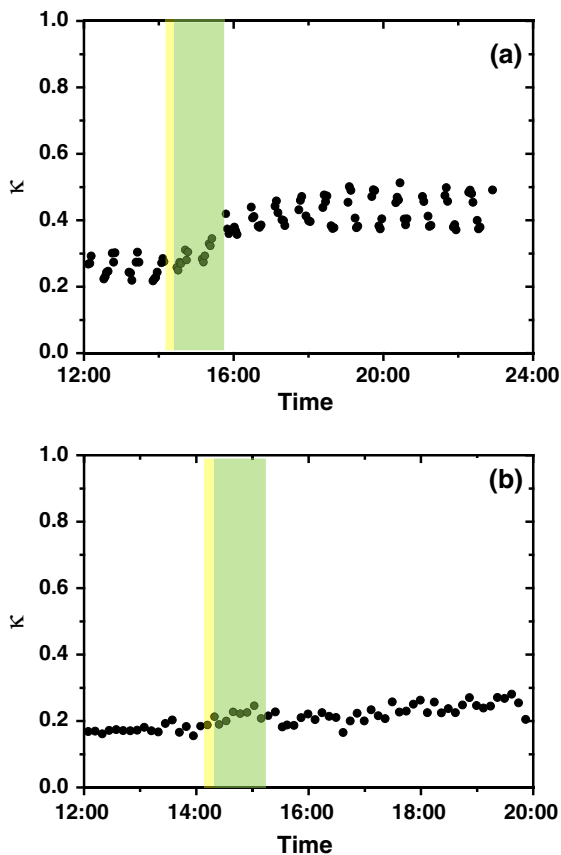


Figure 7

Time series of κ for **a** Experiment 1; **b** Experiment 2. The yellow shadow means **a** HONO and **b** H₂O₂ injection, and the green shadow means the UV light was turned on

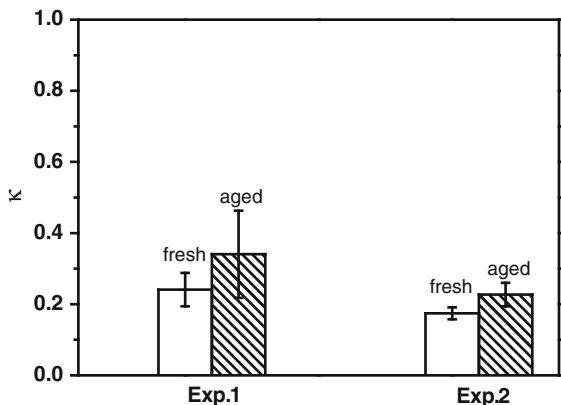


Figure 8

Average κ and its standard deviation for the fresh and aged particles

5. Discussions

Table 1 shows the hygroscopic properties of Saw grass burning particles in other two literatures, along with this study. As shown in Table 1, the fresh burning particles had higher primary κ value of 0.39 in Engelhart et al. (2012) and 0.7 in Petters et al. (2009), while lower κ of 0.21 in our study. The main reason is due to different chemical composition. As discussed (Engelhart et al. 2012), the hygroscopicity should be inversely related to organic fraction and positively correlated with inorganic fraction. In experiment 1 of this study, the organic mass fraction of fresh particles is 89%, much bigger than 35% in Engelhart et al. (2012); the inorganic mass fraction of fresh particles is 3%. With very low inorganic mass and high organic mass, it is not strange that the hygroscopic parameter in our experiment is very low.

After aging, κ of Saw grass burning particles became lower (0.17) in Engelhart et al. (2012) and no results in Petters et al. (2009), while increased 30–42% in our experiments. This can be explained by aging method and chemical composition of aged particles. Engelhart et al. (2012) simulated aging process by only turning on UV lights; while we injected HONO or H₂O₂ before turning on UV lights, which is very representative way of aging in real atmosphere. Different aging process change the chemical composition of the particles differently: either by increase of inorganic mass, decrease of organic mass or increasing the extent of oxidation, the hygroscopic parameter increases.

Hygroscopicity of other biomass burning particles from literature are included in Table 2 with interesting results. The results from Engelhart et al. (2012) and Petters et al. (2009) show that κ of the fresh primary aerosol varied widely; photochemical processing made κ values bigger or smaller for different fuel (Engelhart et al. 2012). Martin et al. (2013) got that the hygroscopicity parameter of aged particles increased generally, consistent with our experiment results. Because of not enough experiments including detailed measurements for aged particles, more studied should be done in the future.

Table 1

Hygroscopic parameter κ of sawgrass inferred from CCN activation data

References	κ		Organic mass fraction		Inorganic mass fraction		O:C	
	Fresh	Aged	Fresh	Aged	Fresh	Aged	Fresh	Aged
Engelhart et al. (2012)	0.39	0.17	0.35	–	–	–	–	–
Petters et al. (2009)	0.7	–	–	–	–	–	–	–
This paper	0.21	0.29	0.9	0.85	0.03	0.12	0.47	0.58

Table 2

Hygroscopic parameter κ of other biomass burning particles inferred from CCN activation data

Fuel	κ		Primary org mass fraction
	Fresh	Aged	
Lodgepole pine	0.1 ^a	0.11 ^a	0.9 ^a
Ponderosa pine	0.1 ^a /0.06 ^b	0.21 ^a	0.95 ^a
Wire grass	0.36 ^a /0.19 ^b	0.1 ^a	0.48 ^a
Turkey oak	0.22 ^a /0.14 ^b	0.11 ^a	0.51 ^a
Galberry	0.06 ^a /0.09 ^b	0.10 ^a	0.88 ^a
Sage	0.50 ^a	0.17 ^a	0.32 ^a
Alaskan duff	0.07 ^a /0.09 ^b	0.07 ^a	0.90 ^a
White spruce	0.10 ^a /0.19 ^b	0.12 ^a	0.76 ^a
Chamise	0.36 ^a /0.33 ^b	0.18 ^a	0.22 ^a
Pocosin	0.09 ^a	0.09 ^a	0.60 ^a
Black spruce	0.07 ^a /0.07 ^b	0.09 ^a	0.85 ^a
Kudzu	0.07 ^b	–	–
Rhododendron	0.08 ^b	–	–
Douglas fir	0.09 ^b	–	–
Manzanita	0.1 ^b	–	–
Hickory	0.14 ^b	–	–
Common reed	0.27 ^b	–	–
Palmetto	0.29 ^b	–	–
Rice straw	0.31 ^b	–	–
Sugar cane	0.32 ^b	–	–
Wax myrtle	0.33 ^b	–	–
Ceanothus	0.4 ^b	–	–
Titi	0.43 ^b	–	–
Beech log wood	0–0.4 ^c	0–0.4 ^c (generally increased)	–

^aFrom Engelhart et al. (2012)^bFrom Petters et al. (2009)^cFrom Martin et al. (2013)

6. Conclusions

The CCN activity and hygroscopic properties of sawgrass burning particles were measured by two smog chamber experiments, and the two experiments suggested that:

1. The fresh particles can serve as reasonable CCN. The average activation diameters at 0.2% supersaturation were 114 and 125 nm, respectively.
2. The aging process changed the chemical composition of the particles. After aging, the fraction of OA decreased by 7 and 5%, NO₃[–] increased by 200 and 190%, and the average O:C ratio

increased by 46 and 11%, respectively in Experiment 1 and 2.

3. The aged particles were more CCN active after aging. The average activation diameters in Experiment 1 and 2 decreased by 8 and 15% at 0.2% supersaturation, respectively.
4. The change in CCN activity for both experiments was consistent with the chemical changes of the particles. The time when the CCN activities changed most was corresponding to the time when chemical composition changed.
5. The hygroscopic parameter κ for the fresh particles were smaller. Chemical aging caused particles more hygroscopic, and κ increased by 42 and 30%, respectively in Experiment 1 and 2.
6. The chemical aging productions were a little different, one was with evident nucleation causing multiple of new particles to form, while the other one did not have evident nucleation, but the CCN activities and hygroscopicity change trends were quite similar.

Acknowledgements

This work was funded by The National Key Research and Development Program (No. 2016YFA0602003) and The National Natural Science Foundation (No. 41275152) of China. Center for Atmospheric Particles Studies (CAPS) of Carnegie Mellon University provided experiment instrumentation. Michael Polen helped to do experiments and edited English. Qing Ye helped to extract the AMS data.

Open Access This article is distributed under the terms of the Creative Commons Attribution 4.0 International License (<http://creativecommons.org/licenses/by/4.0/>), which permits unrestricted use, distribution, and reproduction in any medium, provided you give appropriate credit to the original author(s) and the source, provide a link to the Creative Commons license, and indicate if changes were made.

REFERENCES

- Aiken, A. C., Decarlo, P. F., Kroll, J. H., Worsnop, D. R., Huffman, J. A., Docherty, K. S., et al. (2008). O/C and OM/OC ratios of primary, secondary, and ambient organic aerosols with high resolution time-of-flight aerosol mass spectrometry. *Environmental Science and Technology*, 42, 4478–4485.
- Anderson, B. E., Grant, W. B., Gregory, G. L., Browell, E. V., Collins, J. E., Jr., Sachse, G. W., et al. (1996). Aerosols from biomass burning over the tropical South Atlantic region: Distributions and impacts. *Journal of Geophysical Research*, 101, 24117–24137. <https://doi.org/10.1029/96JD00717>.
- Andreae, M. O. (2009). Correlation between cloud condensation nuclei concentration and aerosol optical thickness in remote and polluted regions. *Atmospheric Chemistry and Physics*, 9, 543–556. <https://doi.org/10.5194/acp-9-543-2009>.
- Andreae, M. O., & Rosenfeld, D. (2008). Aerosol-cloud-precipitation interactions. Part 1. The nature and sources of cloud-active aerosols. *Earth-Science Reviews*, 89, 13–41. <https://doi.org/10.1016/j.earscirev.2008.03.001>.
- Bougiatioti, A., Bezantakos, S., Stavroulas, I., Kalivitis, N., Kokkalis, P., Biskos, G., et al. (2016). Biomass-burning impact on CCN number, hygroscopicity and cloud formation during summertime in the eastern Mediterranean. *Atmospheric Chemistry and Physics*, 16, 7389–7409. <https://doi.org/10.5194/acp-16-7389-2016>.
- Capes, G., Johnson, B., McFiggans, G., Williams, P. I., Haywood, J., & Coe, H. (2008). Aging of biomass burning aerosols over West Africa: Aircraft measurements of chemical composition, microphysical properties, and emission rates. *Journal of Geophysical Research*, 113, D00C15. <https://doi.org/10.1029/2008jd009845>.
- Caseiro, A., Bauer, H., Schmidl, C., Casimiro, A. P., & Puxbaum, H. (2009). Wood burning impact on PM10 in three Austrian regions. *Atmospheric Environment*, 43(13), 2186–2195.
- Cruz, C. N., & Pandis, S. N. (1997). A study of the ability of pure secondary organic aerosol to act as cloud condensation nuclei. *Atmospheric Environment*, 31, 2205–2214.
- Decesari, S., Facchini, M. C., Matta, E., Mircea, M., Fuzzi, S., Chughtai, A. R., et al. (2002). Water soluble organic compounds formed by oxidation of soot. *Atmospheric Environment*, 36(11), 1827–1832.
- Duan, F., Liu, X., Yuc, T., & Cachier, H. (2004). Identification and estimate of biomass burning contribution to the urban aerosol organic carbon concentrations in Beijing. *Atmospheric Environment*, 38(9), 1275–1282.
- Dusek, U., et al. (2005). “Missing” cloud condensation nuclei in peat smoke. *Geophysical Research Letters*, 32, L11802. <https://doi.org/10.1029/2005GL022473>.
- Engelhart, G. J., Asa-Awuku, A., Nenes, A., & Pandis, S. N. (2008). CCN activity and droplet growth kinetics of fresh and aged monoterpene secondary organic aerosol. *Atmospheric Chemistry and Physics*, 8, 3937–3949. <https://doi.org/10.5194/acp-8-3937-2008>.
- Engelhart, G. J., Hennigan, C. J., Miracolo, M. A., Robinson, A. L., & Pandis, S. N. (2012). Cloud condensation nuclei activity of fresh primary and aged biomass burning aerosol. *Atmospheric Chemistry and Physics*, 12, 7285–7293. <https://doi.org/10.5194/acp-12-7285-2012>.
- Favez, O., Cachier, H., Sciare, J., Sarda-Estève, R., & Martinon, L. (2009). Evidence for a significant contribution of wood burning aerosols to PM2.5 during the winter season in Paris, France. *Atmospheric Environment*, 43, 3640–3644.
- Gultepe, I., Heymsfield, A. J., Field, P. R., & Axisa, D. (2017). Ice-phase precipitation. *Meteorological Monographs*, 58, 6.1–6.36.

- Gultepe, I., & Isaac, G. A. (1999). Scale effects on averaging of cloud droplet and aerosol number concentrations: Observations and models. *Journal of Climate*, *12*, 1268–1279.
- Hennigan, C. J., Miracolo, M. A., Engelhart, G. J., May, A. A., Presto, A. A., Lee, T., et al. (2011). Chemical and physical transformations of organic aerosol from the photo-oxidation of open biomass burning emissions in an environmental chamber. *Atmospheric Chemistry and Physics*, *11*, 7669–7686. <https://doi.org/10.5194/acp-11-7669-2011>.
- Hennigan, C. J., Westervelt, D. M., Riipinen, I., Engelhart, G. J., Lee, T., Collett, J. L., Jr., et al. (2012). New particle formation and growth in biomass burning plumes: An important source of cloud condensation nuclei. *Geophysical Research Letters*, *39*, 09805. <https://doi.org/10.1029/2012GL050930>.
- Hobbs, P. V., Sinha, P., Yokelson, R. J., Christian, T. J., Blake, D. R., Gao, S., et al. (2003). Evolution of gases and particles from a savanna fire in South Africa. *Journal of Geophysical Research*, *108*(D13), 8485. <https://doi.org/10.1029/2002JD002352>.
- Jayne, J. T., Leard, D. C., Zhang, X. F., Davidovits, P., Smith, K. A., Kolb, C. E., et al. (2000). Development of an aerosol mass spectrometer for size and composition analysis of submicron particles. *Aerosol Science and Technology*, *33*, 49–70.
- Jimenez, J. L., Jayne, J. T., Shi, Q., Kolb, C. E., Worsnop, D. R., Yourshaw, I., et al. (2003). Ambient aerosol sampling using the aerodyne aerosol mass spectrometer. *Journal of Geophysical Research*, *108*, 8425. <https://doi.org/10.1029/2001JD001213>.
- Kaufman, Y. J., Hobbs, P. V., Kirchhoff, V. W. J. H., Artaxo, P., Remer, L. A., Holben, B. N., et al. (1998). Smoke, Clouds, and Radiation-Brazil (SCAR-B) experiment. *Journal of Geophysical Research*, *103*(D24), 31783–31808.
- Lanz, V., Alfarra, M., Baltensperger, U., Buchmann, B., Hueglin, C., Szidat, S., et al. (2008). Source attribution of submicron organic aerosols during wintertime inversions by advanced factor analysis of aerosol mass spectra. *Environmental Science and Technology*, *42*, 214–220.
- Lee, Y. S., Collins, D. R., Li, R., Bowman, K. P., & Feingold, G. (2006). Expected impact of an aged biomass burning aerosol on cloud condensation nuclei and cloud droplet concentrations. *Journal of Geophysical Research*, *111*, D22204.
- Li, J., Posfai, M., Hobbs, P. V., & Buseck, P. R. (2003). Individual aerosol particles from biomass burning in southern Africa: 2. Composition and aging of inorganic particles. *Journal of Geophysical Research*, *108*(D13), 8448. <https://doi.org/10.1029/2002JD002310>.
- Li, Z. Q., Xia, X., Cribb, M., Mi, W., Holben, B., Wang, P., et al. (2007). Aerosol optical properties and their radiative effects in northern China. *Journal of Geophysical Research*, *112*, D22S01. <https://doi.org/10.1029/2006jd007382>.
- Mallet, M. D., Cravigan, L. T., Milic, A., Alroe, J., Ristovski, Z. D., Ward, J., et al. (2017). Composition, size and cloud condensation nuclei activity of biomass burning aerosol from northern Australian savannah fires. *Atmospheric Chemistry and Physics*, *17*, 3605–3617. <https://doi.org/10.5194/acp-17-3605-2017>.
- Martin, M., Tritscher, T., Juranyi, Z., Heringa, M. F., Sierau, B., Weingartner, E., et al. (2013). Hygroscopicity properties of fresh and aged wood burning particles. *Journal of Aerosol Science*, *56*, 15–29. <https://doi.org/10.1016/j.jaerosci.2012.08.006>.
- Moore, R. H., Nenes, A., & Medina, J. (2010). Scanning mobility CCN analysis—A method for fast measurements of size-resolved CCN distributions and activation kinetics. *Aerosol Science and Technology*, *44*, 861–871.
- Novakov, T., & Corrigan, C. E. (1996). Cloud condensation nucleus activity of the organic component of biomass smoke particles. *Geophysical Research Letters*, *23*(16), 2141–2144. <https://doi.org/10.1029/96GL01971>.
- Onasch, T. B., Trimborn, A., Fortner, E. C., Jayne, J. T., Kok, G. L., Williams, L. R., et al. (2012). Soot particle aerosol mass spectrometer: Development, validation, and initial application. *Aerosol Science and Technology*, *46*(7), 804–817. <https://doi.org/10.1080/02786826.2012.663948>.
- Petters, M. D., Carrico, C. M., Kreidenweis, S. M., Prenni, A. J., DeMott, P. J., Collett, J. L., Jr., et al. (2009). Cloud condensation nucleation activity of biomass burning aerosol. *Journal of Geophysical Research*, *114*, D22205. <https://doi.org/10.1029/2009JD012353>.
- Petters, M. D., & Kreidenweis, S. M. (2007). A single parameter representation of hygroscopic growth and cloud condensation nucleus activity. *Atmospheric Chemistry and Physics*, *7*, 1961–1971.
- Petters, M. D., & Kreidenweis, S. M. (2008). A single parameter representation of hygroscopic growth and cloud condensation nucleus activity—Part 2: Including solubility. *Atmospheric Chemistry and Physics*, *8*, 6273–6279.
- Pierce, J. R., et al. (2007). Contribution of primary carbonaceous aerosol to cloud condensation nuclei: Processes and uncertainties evaluated with a global aerosol microphysics model. *Atmospheric Chemistry and Physics*, *7*, 5447–5466. <https://doi.org/10.5194/acp-7-5447-2007>.
- Pratt, K. A., Heymsfield, A. J., Twohy, C. H., Murphy, S. M., Demott, P. J., Hudson, J. G., et al. (2010). In situ chemical characterization of aged biomass-burning aerosols impacting cloud wave clouds. *Journal of Atmospheric Science*, *67*, 2451e2468.
- Reid, J. S., Koppmann, R., Eck, T. F., & Eleuterio, D. P. (2005). A review of biomass burning emissions part II: Intensive physical properties of biomass burning particles. *Atmospheric Chemistry and Physics*, *5*, 799–825. <https://doi.org/10.5194/acp-5-799-2005>.
- Roberts, G. C., & Nenes, A. (2005). A Continuous-flow streamwise thermal-gradient CCN chamber for atmospheric measurements. *Aerosol Science and Technology*, *39*, 206–221.
- Rose, D., Gunthe, S. S., Mikhailov, E., Frank, G. P., Dusek, U., Andreae, M. O., et al. (2008). Calibration and measurement uncertainties of a continuous-flow cloud condensation nuclei counter (DMT-CCNC): CCN activation of ammonium sulfate and sodium chloride aerosol particles in theory and experiment. *Atmospheric Chemistry and Physics*, *8*, 1153–1179. <https://doi.org/10.5194/acp-8-1153-2008>.
- Rose, D., Nowak, A., Achtert, P., Wiedensohler, A., Hu, M., Shao, M., et al. (2010). Cloud condensation nuclei in polluted air and biomass burning smoke near the mega-city Guangzhou, China—Part 1: Size-resolved measurements and implications for the modeling of aerosol particle hygroscopicity and CCN activity. *Atmospheric Chemistry and Physics*, *10*, 3365–3383. <https://doi.org/10.5194/acp-10-3365-2010>.
- Rosenfeld, D., Dai, J., Yu, X., Yao, Z., Xu, X., Yang, X., et al. (2017). Inverse relations between amounts of air pollution and orographic precipitation. *Science*, *315*, 1396–1398.

- Rosenfeld, D., Lohmann, U., Raga, G. B., O'Dowd, C. D., Kulmala, M., Fuzzi, S., et al. (2008). Flood or drought: How do aerosols affect precipitation? *Science*, *321*, 1309–1313.
- Sandradewi, J., Prevot, A., Szidat, S., Perron, N., Alfarra, M., Lanz, V., et al. (2008). Using aerosol light absorption measurements for the quantitative determination of wood burning and traffic emission contributions to particulate matter. *Environmental Science and Technology*, *42*(9), 3316–3323.
- Spracklen, D. V., et al. (2011). Global cloud condensation nuclei influenced by carbonaceous combustion aerosol. *Atmospheric Chemistry and Physics*, *11*, 9067–9087. <https://doi.org/10.5194/acp-11-9067-2011>.
- Szidat, S., Prevot, A. S. H., Sandradewi, J., Alfarra, M. R., Sýnal, H.-A., Wacker, L., et al. (2007). Dominant impact of residential wood burning on particulate matter in Alpine valleys during winter. *Geophysical Research Letters*, *34*, L05820.
- Twomey, S. (1977). The influence of pollution on the shortwave albedo of clouds. *Journal of Atmospheric Science*, *34*, 1149–1152.
- Vestin, A., Rissler, J., Swietlicki, E., Frank, G. P., & Andreae, M. O. (2007). Cloud-nucleating properties of the Amazonian biomass burning aerosol: Cloud condensation nuclei measurements and modeling. *Journal of Geophysical Research*, *112*, D14201.
- Wu, Z., Zheng, J., Wang, Y., Shang, D., Du, Z., Zhang, Y., et al. (2016). Chemical and physical properties of biomass burning aerosols and their CCN activity: A case study in Beijing, China. *Science of the Total Environment*, *2017*(579), 1260–1268. <https://doi.org/10.1016/j.scitotenv.2016.11.112>. **Epub 2016 Dec 1.**
- Xu, Q. (2001). Abrupt change of the mid-summer climate in central east China by the influence of atmospheric pollution. *Atmospheric Environment*, *35*, 5029–5040.
- Zhao, C., Tie, X., & Lin, Y. (2006). A possible positive feedback of reduction of precipitation and increase in aerosols over eastern central China. *Geophysical Research Letters*, *33*, L11814. <https://doi.org/10.1029/2006GL025959>.
- Zuberi, B., Johnson, K. S., Aleks, G. K., Molina, L. T., Molina, M. J., & Laskin, A. (2005). Hydrophilic properties of aged soot. *Geophysical Research Letters*, *32*, L01807.

(Received October 25, 2017, revised May 3, 2018, accepted May 10, 2018, Published online June 26, 2018)